Photonic crystal ring resonator based add-drop filter using hexagonal rods for CWDM systems

Robinson S* and Nakkeeran R

Department of Electronics and Communication Engineering, Pondicherry Engineering College, Puducherry 605014, India

(Received 21 February 2011)

In this paper, theoretical analysis of two-dimensional photonic crystal ring resonator (2D PCRR) based add-drop filter (ADF) is presented for coarse wavelength division multiplexing (CWDM) system to drop a channel at 1511 nm using hexagonal rods that are positioned in the square lattice. The 2D finite difference time domain (2D FDTD) method and plane wave expansion (PWE) method are used for obtaining the filter response and band structure of the filter respectively. Close to 100% dropping and coupling efficiencies at 1511 nm and 16 nm of bandwidth are observed through simulation. This is very well meeting the requirement of ITU-T G. 694.2 standard, which is specified for metro access and short haul optical networks. The overall size of the proposed filter is 11.4 μm ×11.4 μm. It can also be used in integrated optics.

Document code: A **Article ID:** 1673-1905(2011)03-0164-3

DOI 10.1007/s11801-011-0172-2

The ITU-T G. 694.2 standard was proposed with the eight-channel CWDM system over the wavelength range from 1471 nm to 1611 nm with 20 nm channel spacing for short haul, enterprise and metro access optical networks[1].

Planar lightwave circuit (PLC) and micro electro mechanical system (MEMS) based conventional ADFs, such as Bragg grating based filters, Fabry-Perot filters, arrayed waveguide grating based filters and ring resonator based filters, are all on the scale of centimeters or millimeters[2]. Among these, the ring resonator based ADF provides significant improvement in efficiency because of its circular resonating modes. However, it affects the performance of filter through the presence of radiation and propagation losses. Also the circular resonator is highly sensitive to size when the radius of the ring is reduced to below 5 μm. Hence, it may not be a suitable candidate for photonic integrated circuits (PICs). However, the ADFs designed with photonic crystals (PC) can overcome the above issues and also facilitate the designer to design the devices in the order of micrometers.

Since 1987, photonic crystal (PC) based optical devices have been considered for the design of optical systems with great interest due to their compactness, fast operation speed, long life period and suitability for PICs. Generally, PCs are composed of periodic dielectric or metallo-dielectric nanostructures that have alternate low and high dielectric constant materials (refractive index) in one, two or three dimensions, which affect the propagation of electromagnetic waves inside the structure[3-5]. As a result of this periodicity, it possesses photonic band gap (PBG) where the transmission of light in certain frequency range is absolutely zero. By creating some defects (point or line) in these PBG structures, the periodicity and thus the completeness of the PBG are broken. Thereby the propagation of light can be localized in the PBG region. This can lead to the design of PC based optical devices using the PBG region[5]. Recent years, many PC based optical devices have been theoretically proposed, such as bandstop filters[6], bandpass filters[7,8], channel drop filters[9,10], add-drop filters[11-14] and so on. So far, the square lattice based ADF has been done by introducing point defects and/or line defects[9] using PCRR[10-14]. Generally, the ring resonator based ADF provides efficient wavelength selection, scalability, narrow linewidth, flexible mode design and reduced channel spacing[11]. The ADFs were also designed using square lattice ring resonators, namely square PCRR[11], dual quasi square PCRR[11], quasi square PCRR[11,12], dual curved PCRR[13], and hexagonal PCRR[14].

In this letter, a circular PCRR based ADF is proposed with hexagonal rods embedded in the square lattice structure to meet the requirements of ITU-T G. 694.2 standard. The peculiar property of PC structure is the calculation of PBG which is done by PWE method. The 2D FDTD is used to obtain the coupling and dropping efficiencies of the ADF. The proposed ADF is designed by two dimensional square lattice PCs. The numbers of hexagonal rods in *x* and *z* direc-

* E-mail: mail2robinson@pec.edu

tions are both 21. The distance between the two adjacent rods is 540 nm which is termed as lattice constant and denoted by a. The radius to lattice constant ratio is 0.185 and the silicon (Si) rods are embedded in air substrate. The refractive index of the rod is 2.533 (ε_r=12.482). The values for designing the ADF are chosen from gap map. The gap map gives the rod radius, index contrast and lattice constant with respect to the TE/TM PBG.

Fig.1 shows the band diagram of the PC structure without introducing any defect. It illustrates the propagation modes and PBG of the PC structure. The structure has two PBGs for TE modes and one for TM modes. The normalized frequency of the first reduced PBG starts from $0.42a/\lambda$ to $0.282a/\lambda$ whose corresponding wavelength ranges from 1285 nm to 1914 nm, and that of the second PBG is from $0.7385a/\lambda$ to $0.717a/\lambda$ whose corresponding wavelength ranges from 731.2 nm to 753.1 nm. But the TM band gap occupies the range from $0.835a/\lambda$ to $0.822a/\lambda$ with its wavelength spanning from 646.7 nm to 656.9 nm. Generally, the CWDM network provides optimum performance due to low loss at the third window region of optical communications. Hence, we restrict our attention to the first TE PBG only as its wavelength region coincides with the third window of optical communication.

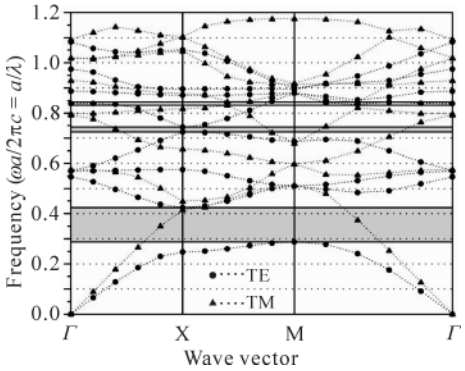

Fig.1 Band diagram of 21×21 PC square lattice structure without introducing any defect

When the defects (line and/or point) are introduced in the periodic structure, the completeness of the PBG is broken and the guided modes (even and odd modes) propagate inside PBG region as shown in Fig.2. The line defects are introduced by removing or changing the shape and size of rods in the row of the entire structure, whereas the point defects are created by changing or removing any rod at specific place in the periodic structure. Here, the line defects for waveguides and point defects for cirular ring cavity are employed. The FDTD method is used to simulate the PC structure and Berenger's perfect matched layer (PML) is placed as absorbing boundary condition[15].

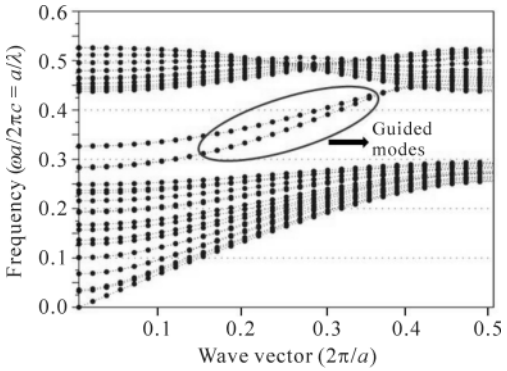

Fig.2 Band diagram of the PC structure after introducing line and point defects

Fig.3(a) and (b) depict the hexagonal rod based resonator and circular PCRR based ADF respectively. The later consists of two waveguides in horizontal (Γ-X) direction and a circular PCRR between them. The top waveguide is called as bus waveguide whereas the bottom waveguide is known as dropping waveguide. The input signal port is marked as A on the left side of the top (bus) waveguide. The ports C and D of bottom (drop) waveguide are the drop terminals and denoted as forward dropping and backward dropping respectively, while the port B of top waveguide is called as the forward transmission terminal. The bus and dropping waveguides are formed by introducing line defects whereas the circular PCRR is shaped by point defects, i.e., removing the column of rods to make a circular shape.

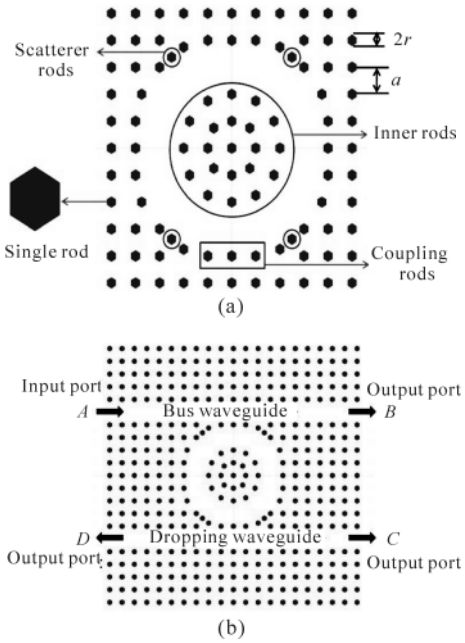

Fig.3 Schematic structures of (a) resonant cavity and (b) circular PCRR based ADF

The circular PCRR is constructed by shifting inner rods

and outer rods of the cavity from their original positions towards center of the origin. The positions of the inner rods, coupling rods and scatterer rods are clearly pictured in Fig.4(a). The scatterer rods are used to reduce the counter propagation modes in order to enhance the coupling and dropping efficiencies, which have similar properties to the other rods.

At resonance, the signal is coupled into the dropping waveguide from bus waveguide and exits through one of the dropping terminals. Here, the coupling and dropping efficiencies are observed by monitoring the power at ports *B* and *C* respectively.

A Gaussian input signal is launched into the input port. The normalized transmission spectra of ports *B*, *C* and *D* are obtained by conducting fast Fourier transform (FFT) of the fields that are calculated by 2D-FDTD method. Fig.4 shows the normalized transmission spectra of ADF. The resonant wavelength at 1511 nm is observed with 16 nm bandwidth. As the bandwidth is 16 nm, it ensures no crosstalk among the CWDM channels. Here, the full width half maximum is considered for bandwidth. The simulation shows 100% coupling and dropping efficiencies which are highly suitable for adding or dropping a single CWDM channel at 1511 nm.

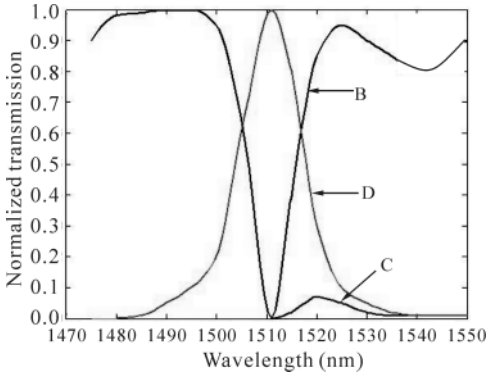

Fig.4 Normalized transmission spectra of circular PCRR based ADF

The Figs.5(a) and (b) depict the electric field patterns of

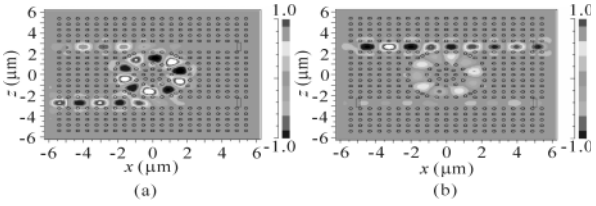

Fig.5 Electric field patterns of the cirular PCRR based ADF at (a) 1511 nm and (b) 1531 nm

pass region and stop region at 1511 nm and 1531 nm, respectively. At resonant wavelength λ=1511 nm, the electric field of the bus waveguide is fully coupled into the ring and reaches the backward dropping terminal. At off resonance λ=1531 nm, the signal directly reaches the transmission terminal without being coupled into the ring.

In conclusion, the circular PCRR based ADF using hexagonal rods is proposed and designed theoretically to add/drop a channel for CWDM systems. The simulation shows 100% coupling efficiency and 100% dropping efficiency at 1511 nm. The proposed ADF is compact and the overall size of the chip is about 11.4 μm × 11.4 μm. Consequently, such devices will be most useful to photonic integrated circuits and CWDM systems for optical networks.

References

[1] International Telecommunication Union, ITU. G. 694.2, 2003.

[2] Dan Sadot and Efraim Boimovich, IEEE Communications Magazine, 50 (1998).

[3] E. Yablonovitch, Phys. Rev. Lett. **58**, 2059 (1987).

[4] S. John, Phys. Rev. Lett. **58**, 2486 (1987).

[5] J. D. Joannopoulos, R. D. Meade and J. N. Winn, Photonic Crystal: Modeling of Flow of Light, Princeton, NJ: Princeton University Press, 2008.

[6] F. Monifi, M. Djavid, A. Ghaffari and M.S. Abrishamian, Proc. PIER, 674 (2008).

[7] M. Djavid, A. Ghaffari, F. Monifi and M. S. Abrishamian, Journal of Applied Science **8**, 1891 (2008).

[8] S. Robinson and R. Nakkeeran, 7th IEEE International Conference on WOCN'10, 2010.

[9] Chun-Chih Wang and Lien-Wen Chen, Physica B **405**, 1210 (2010).

[10] B. S. Darki and N. Granpayesh, Optics Communications **283**, 4099 (2010).

[11] Z. Qiang, W. Zhou and Richard A. Soref, Opti. Express **15**, 1823 (2007).

[12] Juan Jose Vegas Olmos, Masatoshi Tokushima and Kenichi Kitayam, Journal of Selected Topics in Quantum Electronics **16**, 332 (2010).

[13] P. Andalib and N. Granpayeh, 5th IEEE International Conference on Photonics, 249 (2008).

[14] Trong Thi mai, Fu-Li Hsiao, Chengkuo Lee, Wenfeng Xiang, Chii-Chang Chen and W. K. Choi, Sensors and Actuators A: Physical **165**, 16 (2011).

[15] A. Lavrinenko, P. I. Borel, L. H. Frandsen, M. Thorhauge, A. Harpoth, M. Kristensen, T. Niemi and H. M. H. Chong, Opt. Express **12**, 234 (2004).